Intrusive Seismic Swarms as Possible Precursors of Destructive Earthquakes on Mt. Etna's Eastern Flank

Salvatore Gambino (salvatore.gambino@ingv.it)
Istituto Nazionale di Geofisica e Vulcanologia https://orcid.org/0000-0001-8055-3059
Giovanni Distefano
University of Catania: Universita degli Studi di Catania

Full paper

Keywords: Intrusive seismicity, flank dynamics, fault activation, destructive earthquakes

Posted Date: March 22nd, 2021

DOI: https://doi.org/10.21203/rs.3.rs-288277/v1

Version of Record: A version of this preprint was published at International Journal of Geophysics on February 7th, 2022. See the published version at https://doi.org/10.1155/2022/8565536.

Abstract

The Timpe Fault System (TFS) represents the source of shallow earthquakes that strike numerous towns and villages on Mt. Etna eastern flank. In the last 40 years, three destructive seismic events reached I_0 = VIII EMS (heavily damaging) - in 1984 (October 25), 2002 (October 29) and 2018 (December 26). These events followed a few days after the occurrence of strong seismic swarms and the sudden acceleration of the eastern flank seaward. However, if the 2002 and 2018 events were caused by stress induced by eruptive dike propagation, in October 1984 no eruption occurred. In this work, parameters such as localization, cumulative seismic moment and hourly occurrence frequency of the 1984 seismic swarm, have been analyzed and shown to have typical values of Mt. Etna intrusive seismic swarms. This suggests that the 1984 episode may have been an aborted intrusive magma episode that triggered similar processes (long and powerful intrusions with acceleration of the eastern flank movement and destructive earthquakes), as in 2002 and 2018.

These three episodes suggest that an evaluation of some seismic parameters during future intrusive swarms may furnish indications of a possible re-activation of the TFS.

1.0 Introduction

Mt. Etna is a stratovolcano of about 3300 meters, built up over the past 500 ka on the eastern coast of Sicily, and is one of the most active volcanoes on Earth (Fig. 1). At the intersection of two regional structural trends, NE-SW and NNW-SSE oriented (inset in Fig. 1), Mt. Etna is the result of a complex interaction between regional tectonics, flank instability processes and basement geometry (e.g. Bousquet and Lanzafame 2004; Neri et al. 2005).

Volcanic activity on Mt. Etna comprises a persistent activity with episodic paroxysmal events, which occur close to the summit area, and hazardous flank eruptions that are generally preceded by intense intrusive seismic swarms and ground deformation (e.g. Allard et al. 2006).

Its southeastern flank, with an overall area of about 700 km^2, moves ESE seaward continuously, at a rate of a few centimeters per year (e.g. Borgia et al. 1992; Bonforte et al. 2011). This instability is mainly linked to eruptive activity (intrusion and magma pressurization), regional stress and gravitational forces (e.g. Borgia et al. 1992; Acocella et al. 2003; Solaro et al. 2010). The unstable flank is bordered to the north by the Pernicana fault system (PFS) and comprises many active tectonic structures located in the eastern and south-eastern flanks of the volcano, such as the Timpe Fault System (TFS), the Trecastagni and Tremestieri faults (Bonforte et al. 2013), which dissect the eastern flank in different blocks characterized by inhomogeneous kinematics (e.g. Solaro et al. 2010 Azzaro et al. 2013).

PFS moves aseismically but may also be characterized by fast ruptures, generating earthquakes with magnitude up to 4.2 that are closely correlated with acceleration phases of the unstable flank velocity (Alparone et al, 2013a; b). TFS is made up of several fault segments including the Fiandaca (FF), S. Tecla (STF), Moscarello (MOF), Leonardello (SLF) and S. Venerina (SVF) faults (Fig. 1, Fig. 2) characterized by

normal and right-lateral dynamics (Azzaro, 1999; Azzaro et al. 2000; Monaco et al. 1997). These structures normally show right-lateral kinematics and normal dip-slip with slip-rates (3.0 to 5.0 mm/y). However, stress changes due to dike intrusion and accelerations of the southern-eastern flank velocity may cause fast ruptures with displacements up to some tens of centimeters with strong seismic releases (Azzaro, 2004; Walter et al. 2005; Bonforte et al. 2011).

Table 1
List of earthquakes recorded between 1980 and 2019 occurring on Mt. Etna's eastern flank with EMS ≥ 7. EMS = European Macroseismic Scale; Mm = Macroseismic magnitude M_L=Local Magnitude (Azzaro and D'Amico 2019). Bold lines represent the destructive events

	Date	Time (UTC)	Epicentral area	Longitude	Latitude	EMS	*Mm*	M_L
1	20/07/1983	22:03	Viagrande	37.613	15.101	7	4.0	4.3
2	19/06/1984	15:19	Fiandaca	37.636	15.131	7	3.8	4.0
3	19/10/1984	17:43	Zafferana E.	37.698	15.105	7	3.8	4.6
4	**25/10/1984**	**01:11**	**Fleri**	**37.660**	**15.095**	**8**	**4.3**	**4.4**
5	02/02/1986	16:10	S. G. Bosco	37.653	15.163	7	3.8	4.1
6	29/01/1989	07:30	Codavolpe	37.705	15.165	7	3.8	3.4
7	**29/10/2002**	**10:02**	**Bongiardo**	**37.674**	**15.143**	**8**	**4.3**	**4.5**
8	29/10/2002	17:14	Milo	37.717	15.118	7	4.0	3.9
9	**26/12/2018**	**02:19**	**Fleri**	**37.648**	**15.117**	**8**	**4.3**	**4.8**

Earthquakes have magnitudes up to Ml = 4.8 (Colina et al. 2019; Azzaro et al. 2000) and are very shallow, reaching epicentral macroseismic intensity (I_0) up to VIII (heavily damaging) on the EMS (European Macroseismic Scale, Grünthal, 1998), with destructive effects in small areas. In the last 40 years (Table 1 and Fig. 2), only three earthquakes on TFS have reached I_0 = VIII, namely in 1984 (25 October at 01:11 UTC), 2002 (29 October at 10:02 UTC) and 2018 (26 December, 02:19 UTC). These episodes involved the FF (1984 and 2018) and the SVF (2002) structures (Monaco et al. 2005; Azzaro et al. 2006; Civico et al. 2019, Fig. 2).

The 2002 and 2018 events were preceded by significant stress changes due to eruptive dike intrusion that triggered the vigorous eastward movement of the SE flank of Etna with activation of the PFS (Walter et al. 2005; Bonaccorso et al. 2006; Bonforte et al. 2008, De Novellis et al. 2019; Calvari et al. 2020).

The 2002 October 29 earthquake, with a magnitude of Ml = 4.5, produced heavy damage even to reinforced concrete structures in the epicentral area, along a narrow but elongated zone (over 4 km in length) where the macroseismic intensity reached degree VIII (Azzaro et al. 2006; Langer et al. 2016).

The 2018 December 26 earthquake (Ml = 4.8) nucleated on the Fiandaca Fault, characterized by ruptures with perceivable opening and with a right-oblique average slip of 9 cm and a peak value of 35 cm (Civico et al. 2019). Heavy damage due to ground shaking and surface displacement affected buildings, roads and other manmade structures along the fault trace, leaving a thousand people homeless. Surface faulting extended for ~ 8 km (Villani et al. 2020).

For the 2002 and 2018 cases, the relationship between the first cause (intrusion), the cascading effects (flank sliding acceleration, FPS activation) and TFS destructive earthquakes, have been recognized by using the Coulomb stress changes (e.g. Walter et al. 2005, De Novellis et al. 2019).

What happened in 1984 is more difficult to understand for the limited data available. From October 16, an anomalous large number of seismic events, concentrated mostly on the eastern side of the volcano, were recorded for several days on Mt. Etna (Gresta et al. 1987) but no eruption occurred. The main destructive events occurred on October 19 and 25, 1984, with epicentral macroseismic intensity I_0 VII (damaging) and VIII (heavily damaging) EMS respectively, striking the Zafferana territory and especially the villages of Fleri and Pisano (Cannavò et al. 2016). The October 19 event was located in proximity to the Santa Tecla Fault (STF) and showed only small shifts (Alparone and Gambino, 2003, Cannavò et al. 2016) indeed the October 25 earthquake is linked to the Fiandaca Fault (FF) that was affected by ground ruptures of the fault of about 20 cm (Azzaro 1999; Cannavò et al. 2016). At that time, no GPS or InSar measurements were active in order to verify an acceleration of the flank; however, through EDM (Electronic distance measurements) data, Alparone et al. (2013b) showed that a flank sliding acceleration was active from October 1984 until 1986-87.

This paper analyses the 1984 seismicity in order to show how it presents typical features of intrusive seismic swarms at Mt. Etna, suggesting that the 1984 episode may have been an aborted intrusion that caused processes similar to those occurring in 2002 and 2018.

2.0 The October 1984 Seismicity

During the second half of October 1984, an anomalous large number of seismic events, concentrated mostly on the eastern side of the volcano, were recorded on Mt. Etna (Gresta et al. 1987). The main events occurred on October 19 and 25, with epicentral macroseismic intensity I_0 VII and VIII EMS respectively. The first event struck Zafferana Etnea, while to the second are associated the more serious damage in Fleri and Pisano villages and the NW-SE trending cracks along the FF with dip-slip displacements of more than 20 cm (Azzaro 1999; Cannavò et al. 2016).

The seismic swarm was recorded by the permanent seismic network managed by the Catania University. Instrumental investigations of seismicity began at Mt. Etna at the end of the 1960’s with a network that ran for about 30 years and included up to 11 one-component (vertical) stations equipped with 1.0 Hz seismometers (Gresta and Patanè 1987; Gambino et al. 2018).

The swarms started on October the 16th at about 14:00 GMT and ca. 2143 events were recorded until the 31st. The October 1984 swarm is one of the most powerful swarms known on Mt Etna, recording more than 50 events with $M \geq 3.0$ in 15 days. Figure 3 reports the hourly occurrence of earthquakes at the CTS station that evidences two distinct phases of this seismicity: the first, from the 16th at 14:00 to the 18th at 12:00, with a high events occurrence (18.3 events/hours), and a successive phase with an average of about 5 events/hour with a slight increase only close to the 25th. This change occurred after the M = 4.2 earthquakes located on the Pernicana Fault on the 18th at 11:58 GMT.

Of these events about 600 earthquakes with $M > 1.8$ were located by using Hypoellipse (Lahr 1989) and the velocity model of Hirn et al. (1991). These locations are very scattered because they were obtained through manual P and S waves picking on paper seismograms. Therefore, in order to have a more reliable picture of the seismic source locations, data has been considerably reduced by only taking account of the events with more than 7 pickings, RMS > 0.5, GAP > 180°, ERH < 2.5 Km and ERZ < 3.0 Km, obtaining 30 located events for the first phase and 55 for the second one (Fig. 3). The events belonging to the first group are mainly located a few kilometres east with respect to the summit craters, while the events after the 18th at 12:00 are more distributed on the eastern flank of the volcano (Fig. 4).

3.0 The Intrusive Episodes At Mt. Etna

On Mt. Etna, the 1991-93, 2001, 2002, 2008-09 and 2018 eruptions represent the main lateral eruptions occurring over the last 30 years. For each episode, a dike intrusion accompanied by an intense seismic swarm, preceded the opening of eruptive fractures. Indeed, the dike propagation changes the stress field around the intrusion, causing a relevant number of earthquakes that occur close to the dike and activating structures and discontinuities in the nearby areas. This propagation is evidenced by changes in ground deformation measurements, whose modelling allows locating and characterizing the intrusive source (Fig. 5). On Etna, the ability to obtain reliable models began in 1990 with the expansion and improvement of the continuous tilt and GPS permanent networks (Ferro et al. 2011; Gambino et al. 2014; Palano et al. 2010). The 1991-93, 2001, 2002, 2008 and 2018 eruptions have been extensively studied in dozens of papers.

The 1991-93 eruption was characterized by low-explosive activity and produced a very large lava field (total volume of magma of about $235*10^6$ m^3). A shallow intrusion on the upper eastern flank, inferred by Bonaccorso et al, (1996), was accompanied by a seismic swarm of 197 recorded events (Patané et al. 1994) occurring in the same area 5 hours before the fractures opened on December 14, 1991 (Gambino et al. 2018).

The eccentric eruption of 2001 was caused by the forceful uprising of a vertical dike (Bonaccorso et al. 2002; Bonforte et al. 2009) below the south flank (Fig. 5), with magma ascending from a reservoir within the sedimentary substratum (Benchke and Neri 2003). It was preceded by a seismic swarm occurring from July 12 with 2645 events (with M > 1.0) that affected the southern sector southern sector of the

volcano in a main cluster, related to the dike intrusion, with a minor cluster on the upper S-SE sector of the volcano (Patanè et al. 2003; Gambino 2004; Bonforte et al. 2009).

In particular, earthquakes of the main cluster from 13 July to 14 July occurred at a depth between 2.5 and 1.2 km b.s.l. while from 15 July (at 10:00 GMT) seismicity is very shallow (confined at ~ 0.5 km a.s.l.), shifting just below the eruptive fractures (Bonforte et al. 2009).

The 2002–2003 eruption was characterized by a first dike that ascended vertically in the southern flank close to the 2001 eruption site (2002s in Fig. 5) and a second horizontal dike propagating radially in the NE flank, along the NE rift (2002 in Fig. 5). Seismicity started at 20:12 UTC on October 26, 2002. During the first 3–4 h, it took place in the southern-upper part of the volcano when a dike-forming intrusion ascended vertically through the edifice close to the 2001 eruption site (Aloisi et al. 2003; 2006). Successively, the epicentral seismic pattern showed a northeastward migration of earthquakes along the NE Rift with a second dike-forming intrusion propagated laterally along the NE Rift (Aloisi et al. 2006). At 01.28 GMT on 27 October a Md = 3.5 involved the western tip of the Pernicana Fault destroying the Piano Provenzana skiing station (Alparone et al. 2015) and successively an exceptional increase of the seaward movement characterized the eastern flank (Bonaccorso et al. 2006).

The 2008 and 2018 eruptions were characterized by dike intrusions and the opening of lateral eruptive fissures located on the upper eastern flank (Fig. 5).

On May 13, 2008 at 08:40 (GMT), a seismic swarm preceded and accompanied the beginning of the 2008–2009 eruption, when more than 240 events were recorded in about 6–7 h, most of them occurring in the first two hours (Alparone et al., 2012). The eruption started with a fracture system between 3055 m and 2620 m a.s.l. (Aloisi et al. 2009), propagating from the summit craters toward the western wall of the Valle del Bove (e.g. Bonaccorso et al. 2011).

The earthquakes (the largest being ML = 3.9, on May 13, 2008 at 10:07 GMT) were located in the northeastern summit area at depths ranging between 1.5 km b.s.l. and 1.5 km a.s.l. (Alparone et al., 2012). In less than two hours, there was a clear migration of the seismic events toward the north (Patanè 2008), suggesting a propagation of a shallow intrusion toward this sector of the volcano (Aloisi et al. 2009). The intrusion was very fast and was marked by ground deformation recorded at permanent tilt and GPS stations (Aloisi et al. 2009).

In 2018, the eruptive fissures opened at the base of summit craters, with a small lateral eruption though the seismic swarm and ground deformation were very strong. The initial seismicity (December 24 at 8:30 GMT) was located beneath the summit craters and along the eruptive fracture with epicentres aligned in a N-S direction, between − 1 km a. s. l. and 1 km b.s.l. (Alparone et al. 2020) involving the PFS with an ML 3.5 at 10:27 GMT. From 8:30 to 11:10, Aloisi et al. (2020) inferred one propagating magmatic intrusion (2018a in Fig. 5) that ascended near vertically from sea level toward the ground surface where eruptive fissures opened.

However, continuous ground deformation few hours after revealed a new elongated intrusion in the southern flank, matching the southwards migration of seismicity with a deepening of the hypocentres up to 3 km b.s.l. (Alparone et al. 2020) that did not reach the ground surface (2018b in Fig. 5).

After the 24 December 2018 the eastern flank was characterized by strong increased seaward velocity, clearly shown in the slope of the GNSS time series (Mattia et al. 2020).

Therefore, seismic swarms accompanying these five episodes consisted of hundreds of events that took place during the dike propagation and were testified by contemporary ground deformation changes, Table 2 reports some parameters of these seismic episodes (duration, number of events recorded, earthquake hourly frequency and seismic moment).

Table 2

Intrusive seismic swarm parameters. The duration represents the time-interval in which there is contemporaneity between seismicity and ground deformation (Gambino et al, 2018 and references therein; Aloisi et al. 2020; Gruppo Analisi Dati Sismici 2020). The seismic moment Mo was obtained by using (1) and (2) relationships. The 2018 values comprise an estimate of $2.0*10^{15}$ Nm for the 1425 events with M < 1.4 not included in the Bonaccorso and Giampiccolo (2020) calculus. The last row reports data of the first phase of the October 1984 seismic swarm (16th at 14:00-18th at 12:00).

Eruptive episode	***Type***	***Duration (hours)***	***Seismic events (n°)***	***Seismic events (events/hour)***	***Mo (N/m)***
1991-93	Lateral	5.0	197	39.40	4.09E + 15
2001	Eccentric	113.0	2694	23.84	4.35E + 16
2002	Lateral	19.5	294	15.08	1.89E + 16
2008	Lateral	6.4	230	35.94	6.80E + 15
2018	Lateral	31.5	1560	49.52	1.36E + 16
1984	No eruption	43.0	813	18.91	1.55E + 16

On Mt. Etna, the duration of an intrusive process is highly variable, from 5 to 113 hours, while the number of earthquakes ranges between a couple of hundred events to a couple of thousand events with an occurrence between 15 and 50 events/hour. The seismic moment varies within an order of magnitude between ca. $4.0*10^{15}$ Nm and $4.0*10^{16}$ Nm (Gambino et al. 2018; Bonaccorso and Giampiccolo 2020).

In the last row of Table 2 are reported the same parameters obtained for the first phase of the October 1984 seismic swarm (813 events in 43 hours, an hour-frequency of ca. 19 events per hour and an estimated cumulative seismic moment of $1.55*10^{16}$ Nm).

The seismic moment has been obtained with the Giampiccolo et al. (2007) equation:

$\text{Log}(M_o) = (17.60 \pm 0.37) + (1.12 \pm 0.10)*M_L$ (1)

where M_L is the local magnitude of each earthquake that we obtained by converting M_d in M_L using the Tuvè et al. (2015) relationship:

$M_L = 1.164 (\pm 0.011) * M_d - 0.337 ((\pm 0.020)$ (2)

4.0 Discussion And Conclusions

In the last 40 years, three destructive seismic events with I_0 = VIII, have struck the eastern flank of Mt. Etna, namely in 1984 (October 25), 2002 (October 29) and 2018 (December 26), as a result of the re-activation of the FF and SVF structure belonging to TFS.

Several authors have studied the 2002 and 2018 episodes in order to define the causes of the fault activation. In particular, Walter et al. (2005) and Pulvirenti et al. (2017) highlighted that Coulomb stress changes on the SVN, as induced by dike-forming intrusions only, were not sufficient to trigger the October 29, 2002 earthquake. The necessary stress change value is instead reached if we consider the eastern flank movement and the October 27 (01:28 GMT) Pernicana earthquake (Md = 3.5). De Novellis et al. (2019) and Mattia et al. (2020) revealed that the 2018 intrusion prompted, with a positive loading, the seismic activation of FF and other Mt. Etna faults. De Novellis et al. (2019) showed as only the western part of the FF with Coulomb evidenced stress change values up to 0.27 MPa, lower than other faults, for instance the Ragalna Fault reached values up to 0.49 MPa.

In conclusion, these authors have pointed out how the 2002 and 2018 activation of the Timpe Fault System is the combined result of vigorous eruptive intrusions, sudden flank sliding acceleration and PFS activation.

In October 1984 however, no eruption occurred but the seismicity beginning on the 16th showed some common features with intrusive seismic swarms:

1) Location of the 1984 first phase (from the 16th at 14:00 to the 18th at 12:00) is on the high eastern flank of Mt. Etna, similarly to what was observed for other intrusive episodes such as the 1991, 2008 and 2018a events (Fig. 6) involving similar volumes at depths between 1.5 km a.s.l and 2.0 km b.s.l.

2) Seismic parameters, such as hourly seismic events (19 events/hour) and cumulative seismic moment ($1.55*10^{16}$ Nm) are typical of the range of intrusive swarms at Mt Etna (Table 2).

These considerations suggest that the 1984 seismic swarm may be the result of an aborted intrusive magma episode that caused the acceleration of the eastern flank and the destructive earthquakes on TFS (Fig. 7). No eruptive intrusion at Mt. Etna has been recognized during the 2018 eruptions (2018b in Fig. 4), but also in 1989 (Bonaccorso and Davis 1993) and in January 1998 (Bonaccorso and Patanè 2001).

If so, it is interesting to note that the 1984, 2002 and 2018 swarms show common elements, such as:

1) a duration greater than 15–20 hours (Table 2);

2) a cumulative seismic moment (Fig. 8) more than 10^{16} Nm;

3) they are the only episodes that showed a sudden activation of the PFS after a few hours, unlike the 1991, 2001 and 2008 events (Alparone et al. 2013a; b).

It should be emphasized that the 2001 episode, although it shows the highest duration and cumulative seismic moment do not cause significate variations on PFS and on eastern flank sliding. Actually Bonaccorso et al. (2013), by using numerical modeling, already assessed that eccentric intrusions in the south flank, as occurred during the 2001 eruption, do not cause a variation in stress able to promote earthquakes along the PFS. Modeling of GPS measurements instead, reveals that the 2001 intrusion has activated a southward motion of the upper southern part of the volcano (Bonforte et al. 2009).

Therefore, in the last 40 years, we can pinpoint three cases in which strong intrusive seismic swarms are followed by rapid accelerations of the eastern flank (with PFS activation) and occurrence of destructive seismic events on the SVN and FF faults.

The time spans between the start of the intrusive swarm and the strong earthquakes are 1.8 days in 2018, 2.5 days in 2002 and 3.1 for the October 19, 1984 event, while the more destructive (October 25) earthquake occurred after 8.6 days.

Understanding the space-time evolution of eventual strong seismic swarms on the upper eastern and northeastern sectors of Etna is particularly important. If an intrusive seismic swarm occurs (with ground deformations) that extends over time (> 10–15 hours) accumulating a significant seismic moment (> 10^{16} N/m) and activating the PFS, all these elements can be a precursor – a few days ahead - of a fracturing event with strong seismic releases on the TFS.

The results of this work represent a starting point since it considers only three examples that deserve further validation and studies that could in turn lead to realizing an important alert system for those living close to the TFS in the future.

Abbreviations

TFS Timpe Fault System

FF Fiandaca fault

STF Santa Tecla fault

SVF Santa Venerina fault

MOF Moscarello fault

SLF San Leonardello fault

ME Malta Escarpment fault system

MF Messina–Fiumefreddo line

EMS European macroseismic scale

Mo Seismic moment (dyne-cm)

M_L Local magnitude

M_d Duration magnitude

ATL=Aeolian-Tindari-Letojanni

Declarations

- ## Availability of data and materials

The datasets generated during the current study are available from the corresponding author on reasonable request.

- ## Competing interests

The authors have no conflicts of interest to declare that are relevant to the content of this article

- ## Funding

The authors have no relevant financial or non-financial interests to disclose.

- ## Authors' Contributions

SG: data curation, formal analysis, investigation, writing – original draft (lead), review & editing

GD: data curation, formal analysis, investigation.

- ## Acknowledgements

No acknowledgements in this manuscript.

References

1. Acocella V, Behncke B, Neri M, D'Amico S (2003) Link between major flank slip and eruptions at Mt. Etna (Italy). J. Geophys. Res. 30, 2286. doi:10.1029/2003GL018642.

2. Allard P, B. Behncke, S. D'Amico, M. Neri S. Gambino, (2006) Mount Etna 1993-2005: anatomy of an evolving eruptive cycle, Earth-Sci. Rev., 78, 85-114; doi:10.1016/j. earscirev.2006.04.002.
3. Aloisi, M, Bonaccorso, A, Gambino, S, Mattia, M, Puglisi, G, (2003) Etna 2002 eruption imaged from continuous tilt and GPS data. Geophys. Res. Lett., Vol. 30, No. 23, 2214 10.1029/2003GL018896.
4. Aloisi, M, Bonaccorso, A, Gambino, S, (2006) Imaging compositive dike propagation (Etna, 2002 case). J. Geophys. Res. 111, B06404. http://dx.doi.org/10.1029/2005JB003908.
5. Aloisi, M, Bonaccorso, A, Cannavò, F, Gambino, S, Mattia, M, Puglisi, G, Boschi E. (2009) A new dyke intrusion style for the Mount Etna May 2008 eruption modelled through continuous tilt and GPS data. Terra Nova, 21, 316-321.
6. Aloisi M, Bonaccorso A, Cannavò F, Currenti G, Gambino S. (2020) The Dec 24, 2018 eruptive intrusion at Etna volcano as revealed by multi-disciplinary continuous deformation networks (CGPS, borehole strainmeters and tiltmeters) J. Geoph. Res. 125 (8) DOI: 10.1029/2019JB019117.
7. Alparone S, Gambino S, (2003) High precision locations of multiplets on south-eastern flank of Mt. Etna (Italy): reconstruction of fault plan geometry, Physics Earth and Planetary Interiors, 135, 281-289.
8. Alparone S, Barberi G, Cocina O, Giampiccolo E, Musumeci C, Patanè D (2012) Intrusive mechanism of the 2008–2009 Mt. Etna eruption: Constraints by tomographic images and stress tensor analysis, J. Volc. Geoth. Res, 229–230, 50-63, doi:10.1016/j.jvolgeores.2012.04.001.
9. Alparone S, O. Cocina S. Gambino A. Mostaccio S. Spampinato T. Tuvè and A. Ursino, (2013a) Seismological features of the Pernicana-Provenzana fault system and implications for the dynamics of northeastern flank of the volcano, Journal of Volcanology and Geothermal Research, 251, 16-26. doi:10.1016/j.jvolgeores.2012.03.010.
10. Alparone S, A. Bonaccorso A. Bonforte and G. Currenti (2013b) Long-term stress–strain analysis of volcano flank instability: The eastern sector of Etna from 1980 to 2012, J. Geophys. Res. Solid Earth, 118, 5098–5108, doi:10.1002/jgrb.50364.
11. Alparone S, V. Maiolino A. Mostaccio A. Scaltrito A. Ursino, G. Barberi S. D'Amico, G. Di Grazia, E. Giampiccolo C. Musumeci L. Scarfì L. Zuccarello (2015) Instrumental seismic catalogue of Mt Etna earthquakes (Sicily, Italy): ten years (2000–2010) of instrumental recordings. Ann. Geophys., 58 (4) (2015), p. S0435, 10.4401/ag-6591.
12. Alparone S, Barberi, G, Giampiccolo, E, Maiolino, V, Mostaccio, A, Musumeci, C, et al. (2020) Seismological constraints on the 2018 Mt. Etna (Italy) flank eruption and implications for the flank dynamics of the volcano. Terra Nova, 11, 1271–1282. https://doi.org/10.1111/ter.12463
13. Azzaro R. (1999) Earthquake Surface Faulting At Mount Etna Volcano (Sicily) And Implications For Active Tectonics, Journal of Geodynamics, 28 (2-3), 193-213.
14. Azzaro R, Barbano MS, Antichi B, Rigano R, (2000) Macroseismic catalogue of Mt. Etna earthquakes from 1832 to 1998, Acta Vulcanologica, 12 (1-2), 3-36.
15. Azzaro R, (2004) Seismicity and active tectonics in the Etna region: constraints for a seismotectonic model, in Mt. Etna: volcano laboratory, Bonaccorso A, S. Calvari, M. Coltelli, C. Del Negro and S.

Falsaperla (Editors), American Geophysical Union, Geophysical monograph, 143, 205-220.

16. Azzaro, R, S. D'Amico, (2019) Catalogo Macrosismico dei Terremoti Etnei (CMTE). Istituto Nazionale di Geofisica e Vulcanologia (INGV). https://doi.org/10.13127/cmte.
17. Azzaro, R, S. D'Amico, A. Mostaccio, L. Scarfì and Y. Tuvè (2006) Terremoti con effetti macrosismici in Sicilia Orientale - Calabria Meridionale nel periodo Gennaio 2002 – Dicembre 2005, Quaderni di Geofisica, 41, 1-60.
18. Azzaro R, Bonforte A, Branca S, Guglielmino F (2013) Geometry and kinematics of the fault systems controlling the unstable flank of Etna volcano (Sicily). J. Volc. Geotherm. Res.251, 5–15.
19. Behncke, B, Neri, M, (2003) The July-August 2001 eruption of Mt. Etna (Sicily). Bull.Volcanol. 65, 461–476. https://doi.org/10.1007/s00445-003-0274-1.
20. Bonaccorso A, Davis PM (1993) Dislocation of the 1989 dyke intrusion into the flank of Mount Etna, Sicily. J. Geophys. Res. 98, 4261–4268.
21. Bonaccorso A, Ferrucci F, Patanè D, Villari L, (1996) Fast deformation processes and eruptive activity at Mt. Etna (Italy). J. Geophys. Res. 101, 17467–17480.
22. Bonaccorso A, Patanè D (2001) Shear response to an intrusive episode at Mt. Etna volcano (\January 1998) inferred through seismic and tilt data, Tectonoph., 334, 61-75.
23. Bonaccorso A, Currenti G, Del Negro C (2013) Interaction of volcano-tectonic fault with magma storage, intrusion and flank instability: A thirty years study at Mt. Etna volcano. J. Volcanol. Geotherm. Res. 251, 98–111, https://doi.org/10.1016/j.jvolgeores.2012.06.003.
24. Bonaccorso, A, A. Bonforte, F. Guglielmino, M. Palano, and G. Puglisi (2006) Composite ground deformation pattern forerunning the 2004–2005 Mount Etna eruption, J. Geophys. Res, 111, B12207, doi: 10.1029/2005JB004206.
25. Bonaccorso A, Giampiccolo E. (2020) Balance Between Deformation and Seismic Energy Release: The Dec 2018 'Double-Dike' Intrusion at Mt. Etna. Frontiers in Earth Science, 8, 10.3389/feart.2020.583815.
26. Bonforte A, Bonaccorso A, Guglielmino F, Palano M, Puglisi, G (2008) Feeding system and magma storage beneath Mt. Etna as revealed by recent inflation/deflation cycles. J. Geophys. Res. 113, B05406. doi:10.1029/2007JB005334.
27. Bonforte A, Guglielmino F, Coltelli M, Ferretti A, Puglisi, G (2011) Structural assessment of Mt. Etna volcano from Permanent Scatterers analysis. Geochemistry, Geophysics, Geosystems 12, Q02002. http://dx.doi.org/10.1029/2010GC003213.
28. Bonforte A, Carnazzo A, Gambino S, Guglielmino F, Obrizzo F, Puglisi G (2013) A multidisciplinary study of an active fault crossing urban areas: The Trecastagni Fault at Mt. Etna (Italy). Journal of Volcanology and Geothermal Research 02/2013; 251:41-49. DOI:10.1016/j.jvolgeores.2012.05.001.
29. Bonforte A, Gambino S, Neri M (2009) Intrusion of eccentric dikes: The case of the 2001 eruption and its role in the dynamics of Mt. Etna volcano. Tectonophysics, 471, 1-2, 78-86.

30. Borgia A, Ferrari L, Pasquarè G (1992) Importance of gravitational spreading in the tectonic and volcanic evolution of Mount Etna. Nature, 357(6375), 231–235. https://doi.org/10.1038/357231a0.
31. Bousquet JC, Lanzafame G (2004) The tectonics and geodynamics of Mt. Etna: Synthesis and interpretation of geological and geophysical data, in Etna Volcano Laboratory, Geophys. Monogr. Ser., vol. 143, edited by A. Bonaccorso, S. Calvari, M. Coltelli, C. Del Negro, and S. Falsaperla, pp. 29–47, AGU, Washington, D.C.
32. Calvari S, Bilotta G, Bonaccorso A, Caltabiano T, Cappello A, Corradino C, Del Negro C, Ganci G, Neri M., Pecora E, Salerno G, Spampinato L (2020) The VEI 2 Christmas 2018 Etna Eruption: A Small but Intense Eruptive Event or the Starting Phase of a Larger One? Remote Sens., 12, 905.
33. Cannavò F, Gambino G, Puglisi B, Velardita, R (2016) Modeling ground deformation associated with the destructive earthquakes occurring on Mt. Etna's southeastern flank in 1984. Nat. Hazards Earth Syst. Sci., 16, 2443–2453.
34. Civico R, Pucci S, Nappi R, Azzaro R, Villani F, Pantosti, D, et al. (2019) Surface ruptures following the 26 December 2018, Mw 4.9, Mt. Etna earthquake, Sicily (Italy). Journal of Maps, 15(2), 831–837. https://doi.org/10.1080/17445647.2019.1683476.
35. De Novellis, V, Atzori, S, De Luca, C, Manzo, M, Valerio, E, Bonano, M, et al. (2019) DInSAR analysis and analytical modeling of Mount Etna displacements: The December 2018 volcano-tectonic crisis. Geophysical Research Letters, 46, 5817–5827. https://doi.org/10.1029/2019GL082467.
36. Ferro A, Gambino S, Panepinto S, Falzone G, Laudani G. Ducarme B (2011) High precision tilt observation at Mt. Etna Volcano, Italy. Acta Geophysica, 59, 3, 618-632.
37. Gambino S (2004) Continuous dynamic response along a pre-existing structural discontinuity induced by the 2001 eruption at Mt Etna. Earth Planets Space, 56, 447-456.
38. Gambino, S, Falzone, G, Ferro, A, Laudani G (2014) Volcanic processes detected by tiltmeters: A review of experience on Sicilian volcanoes. Journal of Volcanology and Geothermal Research 271. DOI:10.1016/j.jvolgeores.2013.11.007
39. Gambino S, Distefano G, Maiolino V, Gresta S (2018) Seismic vs. geodetic moments at Mt. Etna volcano: A tool for a rapid understanding of eruptive behaviour? J. Volc. Geoth. Res., 367, 1-6.
40. Gresta, S, Glot, J.P, Patanè, G, Poupinet, G, Menza, S (1987) The October seismic crisis at Mount Etna. Part I: Space-Time evolution of events. Ann. Geophys. 5B (6), 671–680.
41. Gresta, S, Patanè, D (1987) Review of seismological studies at Mount Etna. Pure Appl. Geophys. 125, 951–970
42. Grünthal, G. (eds) (1998) European macroseismic scale 1998 (EMS-98). European Seismological Commission, subcommission on Engineering Seismology, working Group Macroseismic Scales. Conseil de l'Europe, Cahiers du Centre Européen de Géodynamique et de Séismologie, 15, Luxembourg, 99 pp.
43. Gruppo Analisi Dati Sismici (2020) Catalogo dei terremoti della Sicilia Orientale - Calabria Meridionale (1999-2020). INGV, Catania http://sismoweb.ct.ingv.it/maps/eq_maps/sicily/catalogue.php.

44. Hirn, A, A. Nercessian, M. Sapin, F. Ferrucci, Wittlinger G (1991) Seismic heterogeneity of Mt. Etna: structure and activity, Geophys. J. Int., 105, 139–153.
45. Lahr JC (1989) Hypoellipse Version 2.0*: a computer program for determining local earthquake hypocentral parameters, magnitude, and first motion pattern. United States Department of the Survey Menlo Park, California, Open File Report, 89–116.
46. Langer H, Tusa G, Scarfì L, Azzaro R (2016) Ground-motion scenarios on Mt. Etna inferred from empirical relations and synthetic simulations. Bull Earthquake Eng 14:1917–1943, 10.1007/s10518-015-9823-1.
47. Mattia M, Bruno V, Montgomery-Brown E, Patanè D, Barberi G, Coltelli M (2020) Combined seismic and geodetic analysis before, during, and after the 2018 Mount Etna eruption. Geochemistry, Geophysics, Geosystems, 21, e2020GC009218. https://doi.org/10.1029/2020GC009218.
48. Monaco C, Tapponnier P, Tortorici L. Gillot PY (1997) Late Quaternary slip-rates on the Acireale-Piedimonte fault system and tectonic origin of Mt. Etna. Earth and Planetary Science Lett, 147, 125-139.
49. Monaco C, Catalano S, Cocina O, De Guidi G, Ferlito C, Gresta S, Musumeci C, Tortorici L (2005) Tectonic control on the eruptive dynamics at Mt. Etna volcano (eastern Sicily) during the 2001 and 2002-2003 eruptions. J. Volc. Geoterm. Res., 144, 221-233.
50. Neri, M, Acocella, V, Behncke, B, Maiolino, V, Ursino, A, Velardita, R (2005) Contrasting triggering mechanisms of the 2001 and 2002–2003 eruptions of Mount Etna (Italy). J. Volcanol. Geotherm. Res. 144, 235–255.
51. Palano M, Rossi, M, Cannavò F, Bruno V, Aloisi M, Pellegrino D, Pulvirenti M, Siligato G, Mattia M (2010) Etn@ref: a geodetic reference frame for Mt. Etna GPS networks Annals of Geophysics, 53, p. 4, 10.4401/ag-4879.
52. Patané, D, E. Privitera, F. Ferrucci, S. Gresta, S, (1994) Seismic activity leading to the 1991-1993 eruption of Mt. Etna and its implications, Acta Vulcanologica 4, 47-55.
53. Patanè D, et al. (2003) Seismological constraints for the dike emplacement of July-August 2001 lateral eruption at Mt. Etna volcano, Italy. Ann. Geophys., 46, 599-608.
54. Patanè D (2008) Quadro di sintesi e aggiornamento al 19 Maggio 2008 sullo stato di attività sismica dell'Etna, INGV internal report WKRSM20080519, http://www.ct.ingv.it/Etna2007/main.htm.
55. Pulvirenti F, M. Aloisi, Jin S (2017) Time-dependent Coulomb stress changes induced by the 2002–2003 Etna magmatic intrusions and implications on following seismic activities J. Volcanol. Geotherm. Res., 344, pp. 185-196.
56. Solaro G, V. Acocella, S. Pepe, J. Ruch, M. Neri, Sansosti E. (2010) Anatomy of an unstable volcano from InSAR: Multiple processes affecting flank instability at Mt. Etna, 1994-2008, Journal of Geophysical Research, 115, B10405, doi:10.1029/2009JB000820.
57. Tuvè T, D'Amico S, Giampiccolo E (2015) A new Md-ML relationship for Mt. Etna earthquakes (Italy). Ann. Geophys. 58, 6. https://doi.org/10.4401/ag-6830S0657.

58. Villani, F. et al. (2020) Surface ruptures database related to the 26 December 2018, M-W 4.9 Mt. Etna earthquake, southern Italy. Scientific Data https://doi.org/10.1038/s41597-020-0383-0.
59. Walter TR, Acocella V, Neri M, Amelung F (2005) Feedback processes between magmatic events and flank movement at Mount Etna (Italy) during the 2002–2003 eruption. Journal of Geophysical Research, 110, B10205. https://doi.org/10.1029/2005JB003688.

Figures

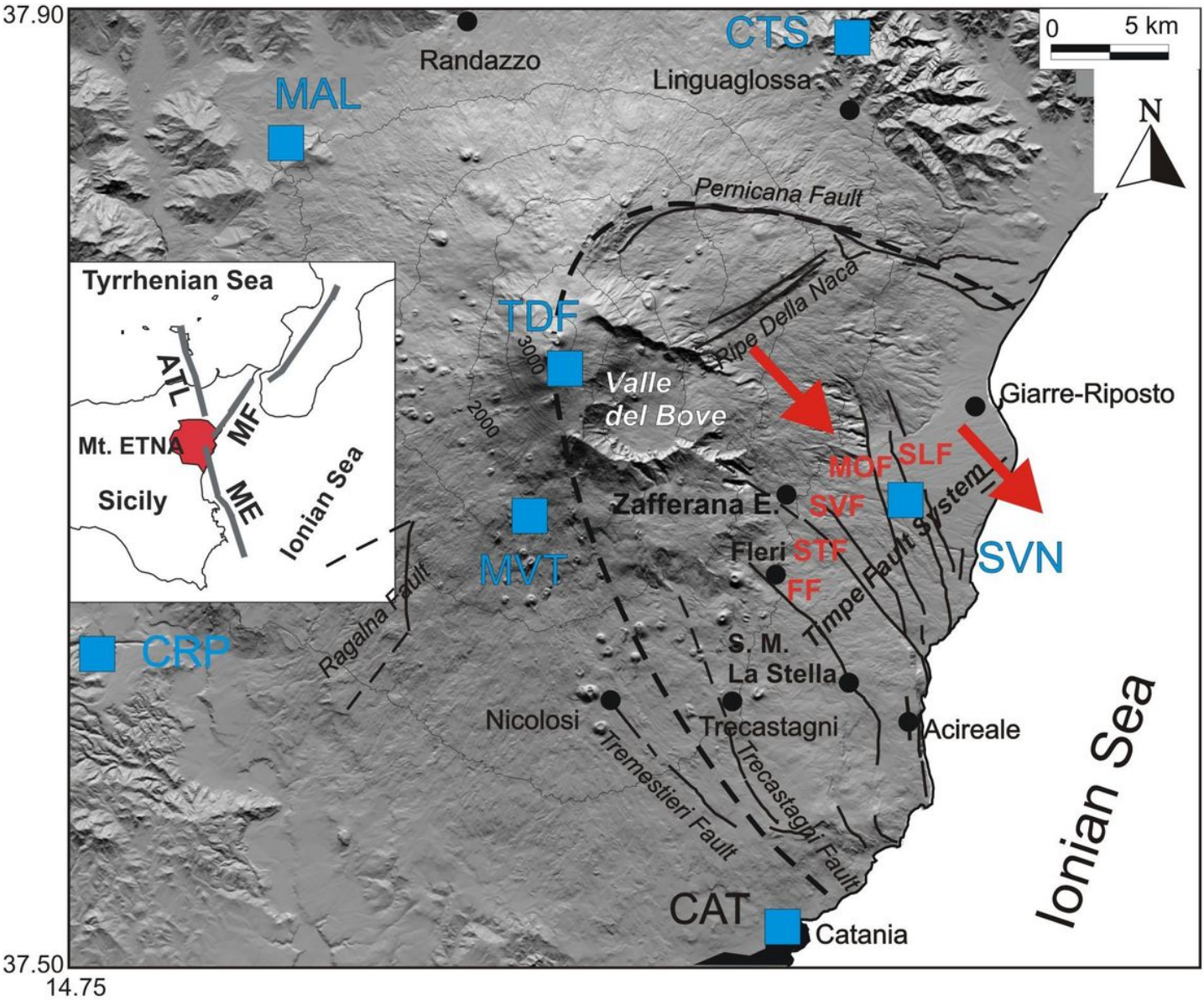

Figure 1

Surface faults map of Mt. Etna. Top inset map shows the main regional fault systems: MF=Messina-Fiumefreddo, ME=Malta Escarpment, ATL=Aeolian-Tindari-Letojanni. Dashed line defines the sliding sector and red arrows indicate its movement direction. FF=Fiandaca fault, STF=Santa Tecla fault, SVF=Santa Venerina fault, MOF=Moscarello fault and SLF=San Leonardello fault. Blue squares show seismic stations of the University of Catania network operating on Etna in 1984. Note: The designations employed and the presentation of the material on this map do not imply the expression of any opinion whatsoever on the part of Research Square concerning the legal status of any country, territory, city or area or of its authorities, or concerning the delimitation of its frontiers or boundaries. This map has been provided by the authors.

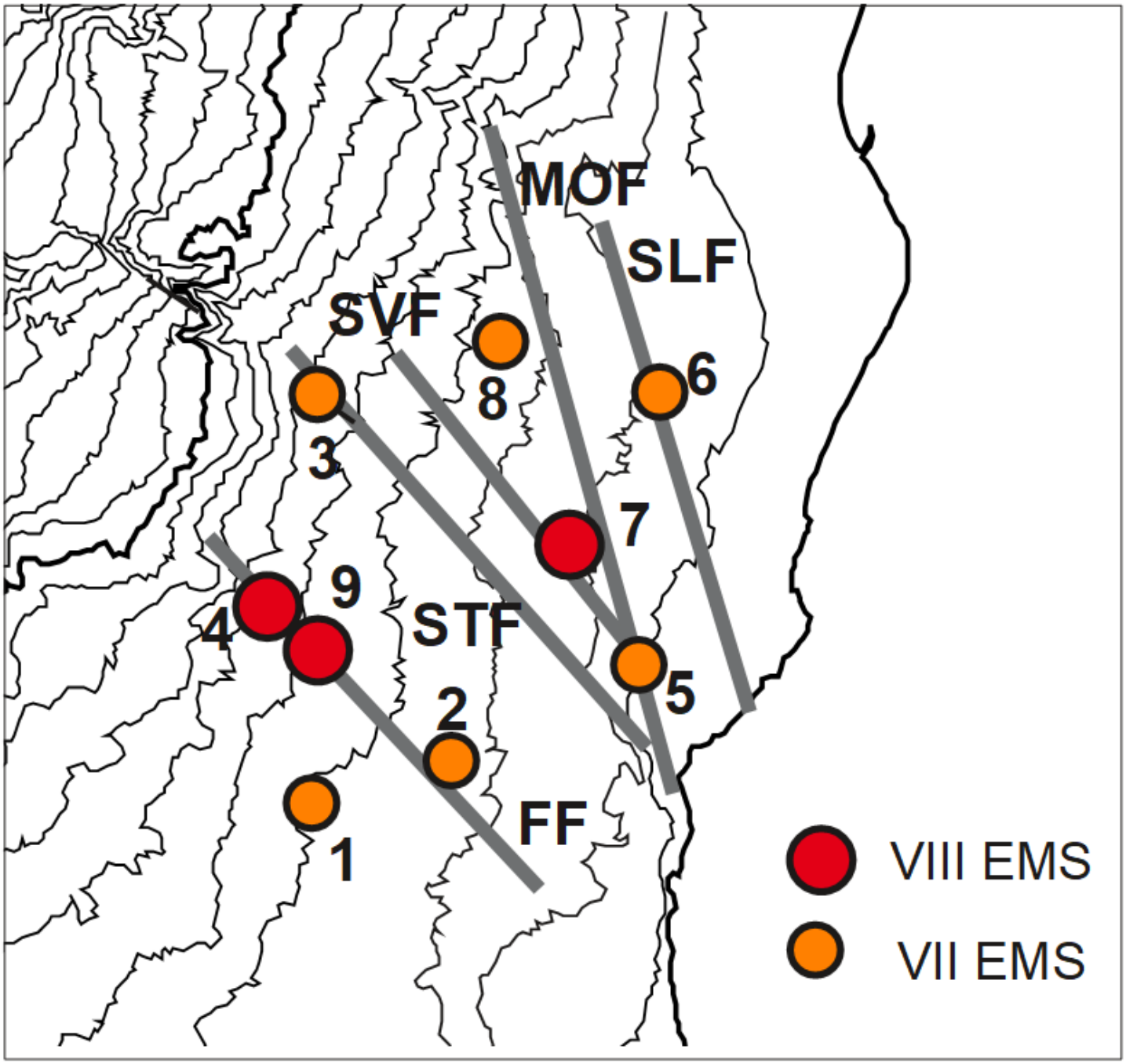

Figure 2

Macroseismic location of earthquakes with epicentral intensities Io ≥ VII EMS occurring from 1980 to 2019 in the southeastern flank of Mt. Etna (Azzaro and D'Amico 2019). Numbers are referred to Tab. 1. Note: The designations employed and the presentation of the material on this map do not imply the expression of any opinion whatsoever on the part of Research Square concerning the legal status of any country, territory, city or area or of its authorities, or concerning the delimitation of its frontiers or boundaries. This map has been provided by the authors.

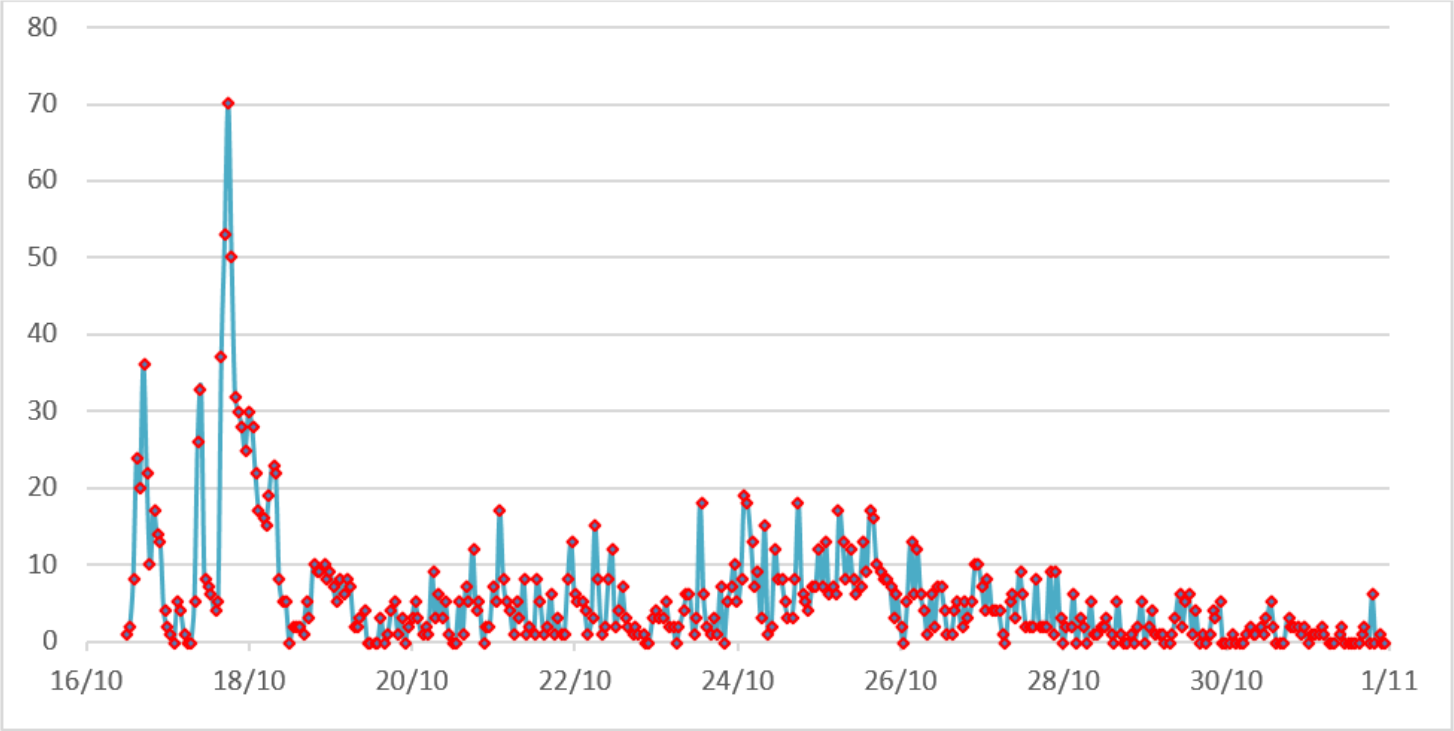

Figure 3

Earthquakes hourly frequency at CTS station from October 16 to October 31.

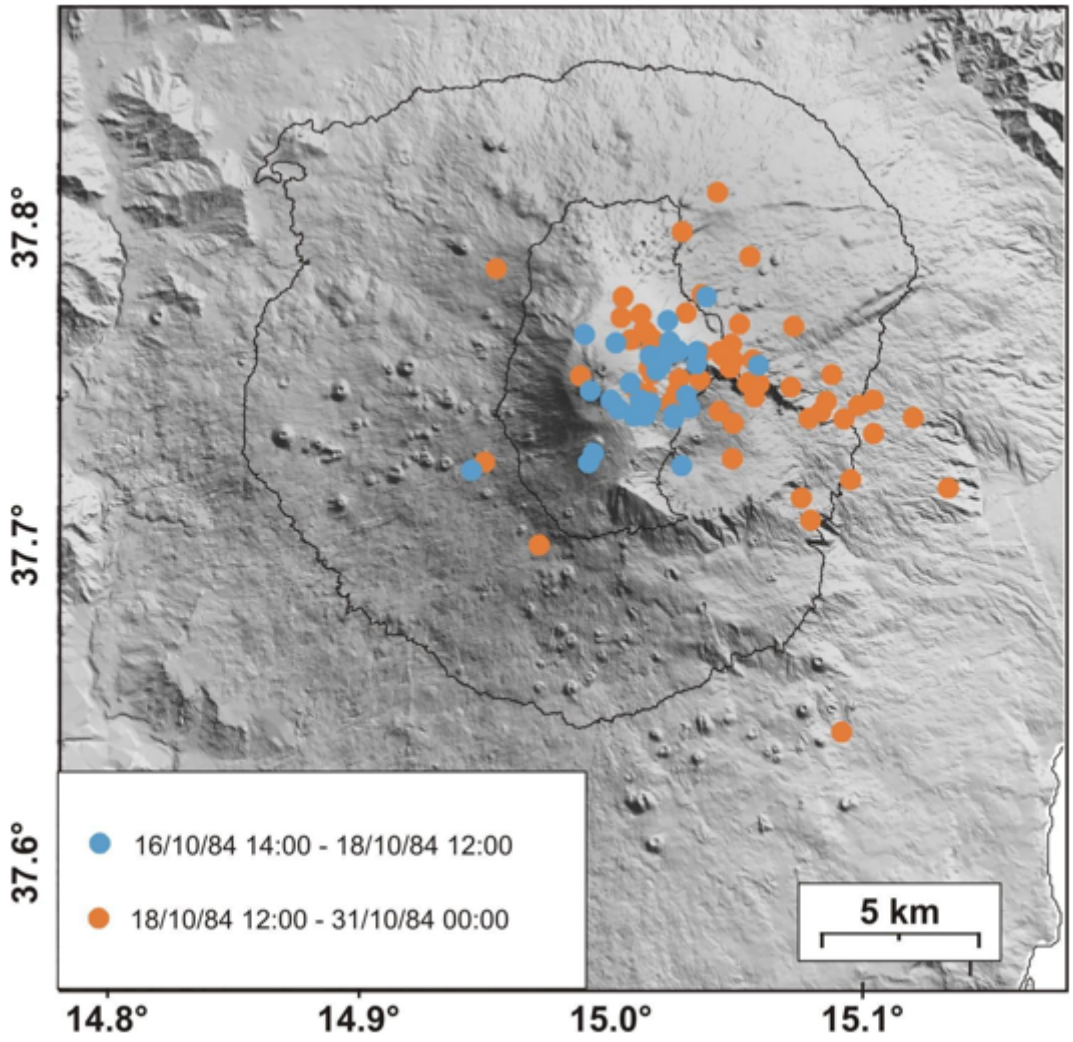

Figure 4

Epicentral location of selected earthquakes for the first (blue) and second (orange) phase. Note: The designations employed and the presentation of the material on this map do not imply the expression of any opinion whatsoever on the part of Research Square concerning the legal status of any country, territory, city or area or of its authorities, or concerning the delimitation of its frontiers or boundaries. This map has been provided by the authors.

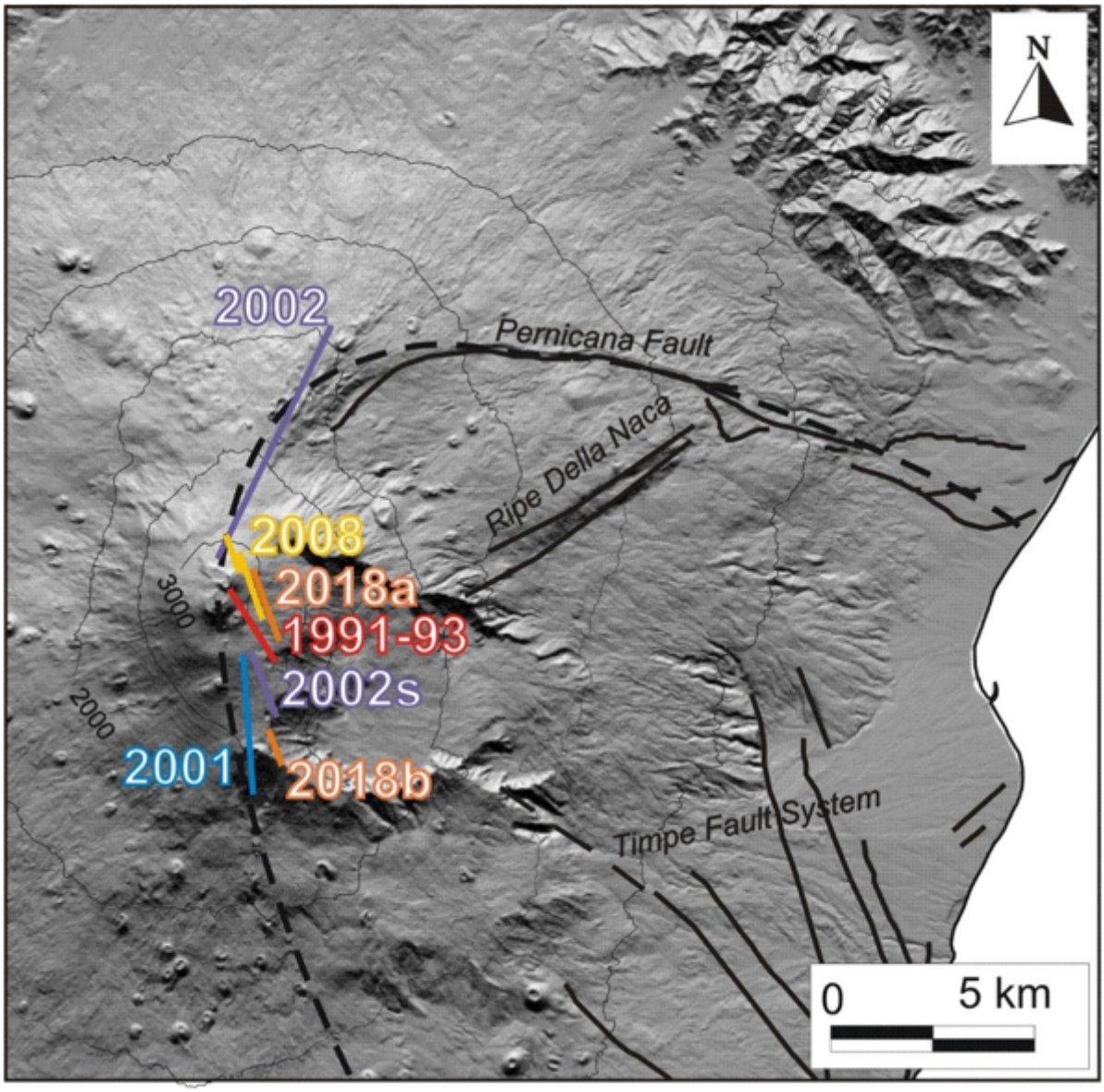

Figure 5

Map showing the eruptive dike intrusive sources obtained by modelling tilt and GPS ground deformation data (Bonaccorso et al, 1996; Bonforte et al. 2009, Aloisi et al. 2006, 2009, 2020). Note: The designations employed and the presentation of the material on this map do not imply the expression of any opinion whatsoever on the part of Research Square concerning the legal status of any country, territory, city or area or of its authorities, or concerning the delimitation of its frontiers or boundaries. This map has been provided by the authors.

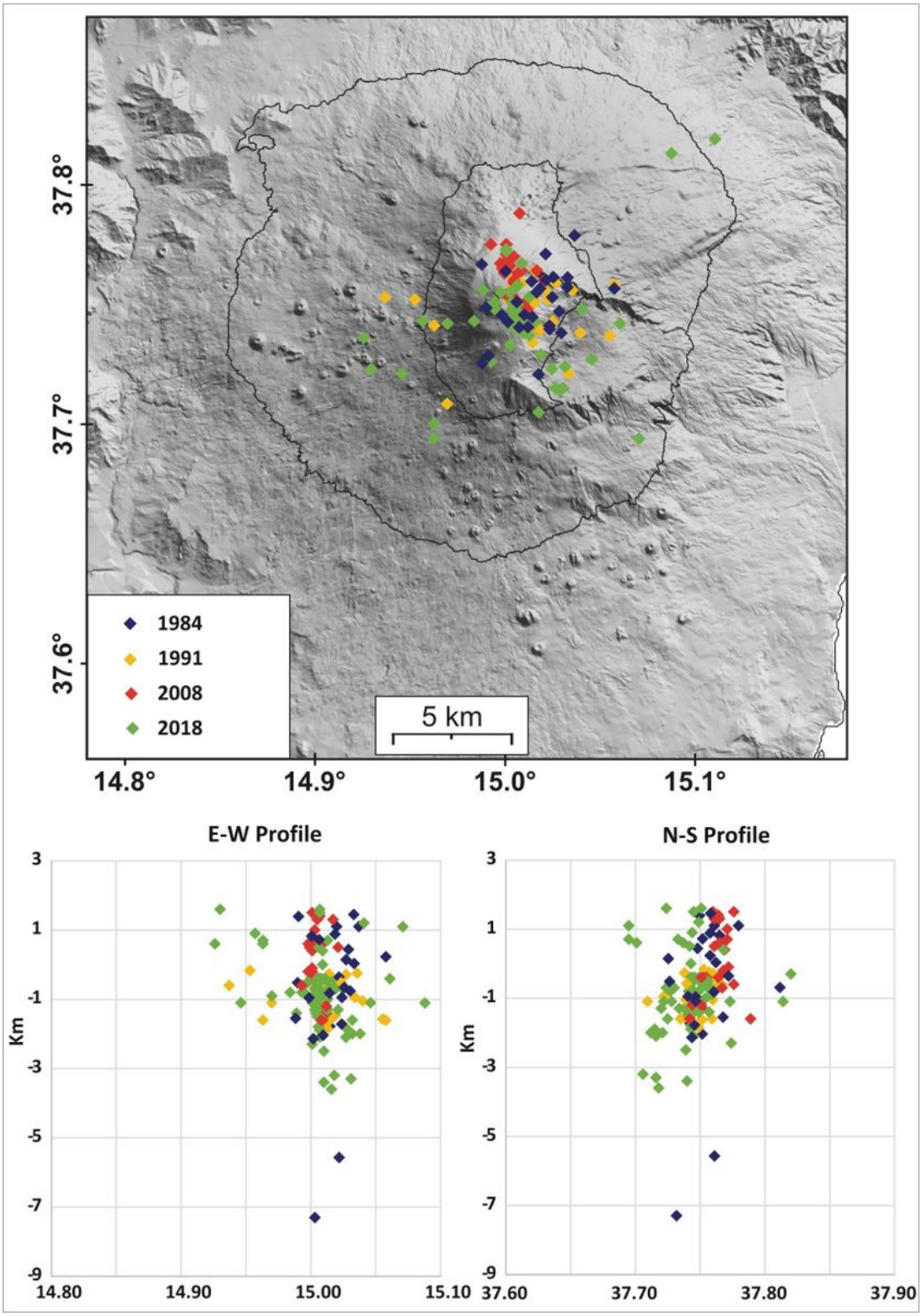

Figure 6

Map and cross sections of the located seismicity recorded during the 1984, 1991, 2008 and 2018a intrusive phases. Note: The designations employed and the presentation of the material on this map do not imply the expression of any opinion whatsoever on the part of Research Square concerning the legal status of any country, territory, city or area or of its authorities, or concerning the delimitation of its frontiers or boundaries. This map has been provided by the authors.

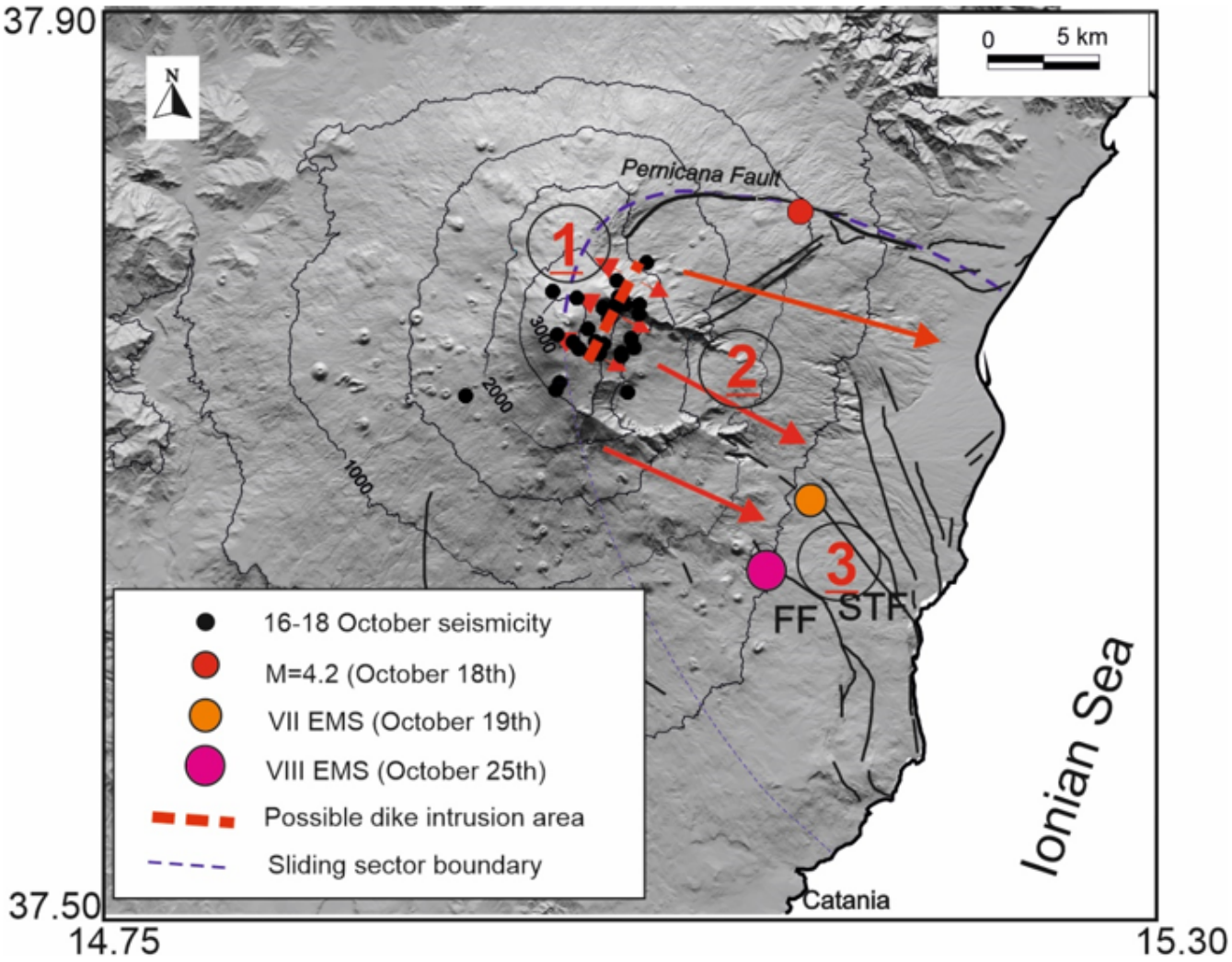

Figure 7

Sequence of the events occurred in October 1984: 1) the seismic swarm is the result of an aborted magmatic intrusion that caused 2) the acceleration of the eastern flank (with PFS activation) and 3) the destructive earthquakes on TFS. Note: The designations employed and the presentation of the material on this map do not imply the expression of any opinion whatsoever on the part of Research Square concerning the legal status of any country, territory, city or area or of its authorities, or concerning the delimitation of its frontiers or boundaries. This map has been provided by the authors.

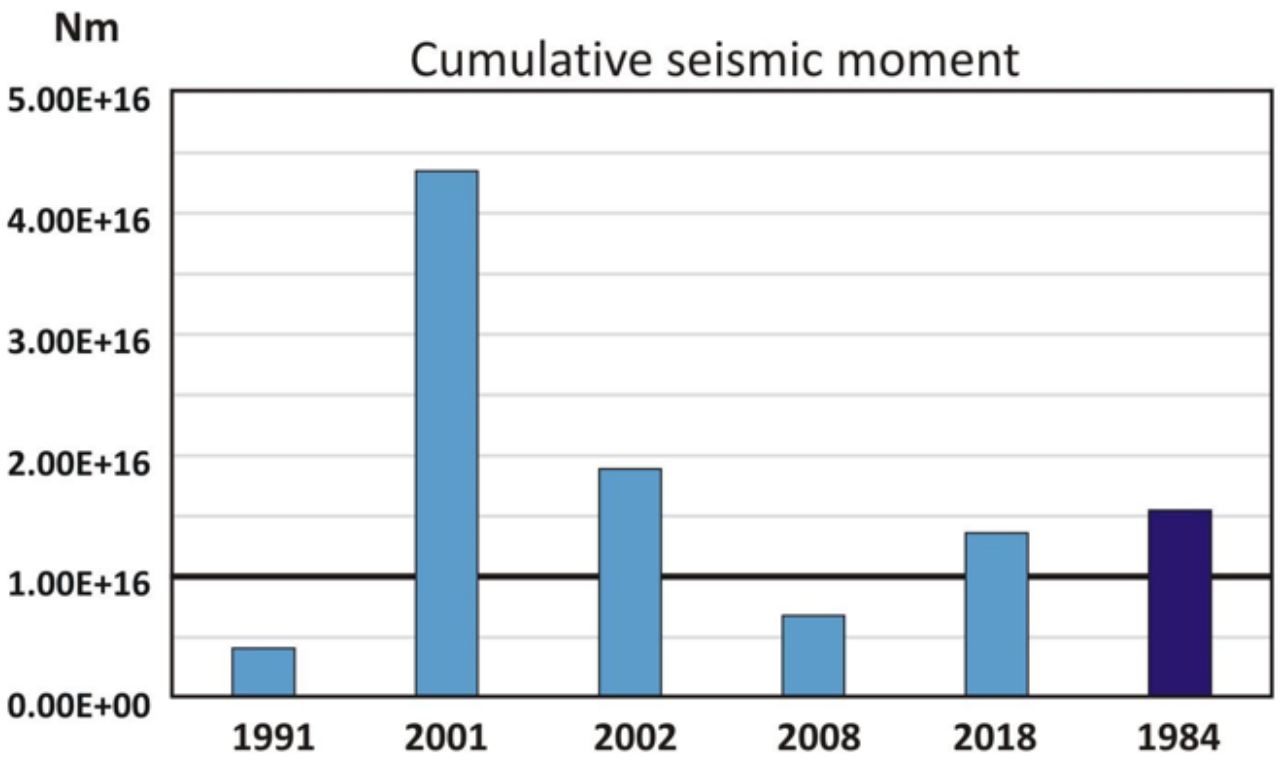

Figure 8

Cumulative seismic moment obtained for the intrusive seismic swarms.

Supplementary Files

This is a list of supplementary files associated with this preprint. Click to download.

- FIGURAFINALE.jpg